Original Article

Inhibitors of HIV-1 integrase from *Dioscorea bulbifera*

Prapaporn Chaniad[1], Chatchai Wattanapiromsakul[1,2], Somsak Pianwanit[3], and Supinya Tewtrakul[1,2*]

[1] Department of Pharmacognosy and Pharmaceutical Botany,

[2] Excellent Research Laboratory, Phytomedicine and Pharmaceutical Biotechnology Excellence Center,
Faculty of Pharmaceutical Sciences,
Prince of Songkla University, Hat Yai, Songkhla, 90112 Thailand.

[3] Department of Chemistry, Faculty of Science,
Chulalongkorn University, Pathum Wan, Bangkok, 10330 Thailand.

Abstract

A search for HIV-1 integrase (IN) inhibitors from natural sources has led to the isolation of compounds from *Dioscorea bulbifera* bulbils. From the bioassay-guided isolation, the chloroform fraction was then fractionated to obtain one new clerodane diterpenoid (diosbulbin E acetate, **4**), two known clerodane diterpenoids (**1-2**), four flavonoids (**5-8**) and one sterol glucoside (**3**). Quercetin (**7**) exhibited the strongest anti-HIV-1 IN activity with an IC_{50} value of 16.28 μM, followed by kaempferol (**8**, $IC_{50} = 37.71$ μM), whereas (+)-catechin (**6**) possessed moderate activity ($IC_{50} = 62.36$ μM). Moreover, the clerodane-type diterpenoids (**1** and **4**) also exhibited moderate inhibitory effects with IC_{50} values of 70.39 and 73.49 μM, respectively. The flavonoid compounds (**5-8**) were also investigated for their interactions with the IN active sites using a molecular docking method. They interacted with Thr66, His67, Gln148, Glu152 and Lys159, which are important amino acid residues for inhibition of HIV-1 IN activity.

Keywords: anti-HIV-1 integrase activity, *Dioscorea bulbifera* L., molecular docking, diosbulbin E acetate, clerodane diterpenoid

1. Introduction

Acquired immune deficiency syndrome (AIDS) is caused by human immunodeficiency virus (HIV). HIV-1 integrase (IN) is an essential enzyme for viral replication. It catalyzes the insertion and integration of reverse transcribed viral DNA into the host genome. The full length HIV-1 IN contains 288 amino acids and consists of three functional domains. They are the N-terminal domain (residues 1-49), the catalytic core domain (residues 50-212) and the C-terminal domain (residues 213-288). The N-terminal domain contains a His-His-Cys-Cys zinc finger-like motif. The catalytic core domain is characterized by three catalytic residues (Asp64, Asp116, and Glu152) that can bind divalent cations such as Mg^{2+} or Mn^{2+}. The C-terminal domain is less conserved and is responsible for the nonspecific recognition of DNA (Katz and Skalka, 1994; Camarasa *et al.*, 2006). The integration process is catalyzed by the IN through two consecutive catalytic reactions referred to as 3′-processing and DNA strand transfer (Asante-Appiah and Skalka, 1997). Nowadays, there are only three HIV-1 IN inhibitors, raltegravir, elvitegravir and dolutegravir, that have been approved by the Food and Drug Administration (Clercq, 2009; Saag, 2012). Moreover, IN has no human counterpart, making it a very attractive target to

---

* Corresponding author.
  Email address: supinyat@yahoo.com; supinya.t@psu.ac.th

develop new anti-HIV drugs, especially the search for HIV-1 IN inhibitors from natural sources has become an interesting approach.

Dioscorea bulbifera L. (Dioscoreaceae) is a medicinal plant in Thai traditional longevity preparations, and locally known in Thai as Wan Phra Chim. Various extracts of bulbils possess various biological activities, such as an analgesic, anti-inflammatory (Mbiantcha *et al.*, 2011), antitumor (Wang *et al.*, 2012), antihyperglycemic and antidyslipidemic activities (Ahmed *et al.*, 2009). It is important to note that there have been no reports for any anti-HIV-1 IN activity from *D. bulbifera* until now. In our study, an ethanol extract of *D. bulbifera* bulbils possessed high anti-HIV-1 IN activity with an IC_{50} of 9.3 µg/mL. Therefore, this study aimed to isolate the compounds and to test them for anti-HIV-1 IN activity using the multiplate integration assay (MIA), as well as to investigate the interaction of the active compounds with IN using a molecular docking method.

2. Materials and Methods

2.1 Enzyme and chemicals

The HIV-1 IN enzyme was purified according to the method described by Goldgur *et al.* (1999). Oligonucleotides of the long terminal repeated bases from the donor DNA and from the target substrate DNA were purchased from QIAGEN Operon, USA, and stored at -25°C before use. All other chemicals used were of analytical grade from Sigma Aldrich, USA.

2.2 Plant material

D. bulbifera bulbils were collected from Uttaradit province, Thailand, in 2011. The plants were identified by a botanist of the Forest Herbarium, Department of National Parks, Wildlife and Plant Conservation, Thailand. Voucher specimen (SKP 062040201) is deposited in Faculty of Pharmaceutical Sciences, Prince of Songkla University.

2.3 Extraction and isolation of compounds from *D. bulbifera* extract

The bulbils powder (1.7 kg) was extracted three times with ethanol (3×15 L) at room temperature. The crude ethanol extract was evaporated to dryness under vacuum at 45°C and 258.0 g of dry powder was obtained (15.1% w/w). This extract was successively partitioned to obtain chloroform (108.15 g), ethyl acetate (44.44 g) and water fractions (105.18 g), respectively.

Based on the bioassay-guided isolation of active compounds that possessed anti-HIV-1 IN activity, the chloroform fraction exhibited the highest activity with an IC_{50} value of 5.42 µg/mL (Table 1). Therefore, this fraction was further selected to isolate the active compounds. The chloroform fraction (60.00 g) was separated by vacuum liquid chromatography (VLC) using silica gel and eluted with chloroform then with ethyl acetate and methanol for an increasing polarity. Similar fractions were combined by TLC monitoring to obtain 7 fractions (A-G). Fraction A (8.07 g) was further separated by VLC and eluted with chloroform/methanol (0-50%) to give six subfractions (A1-A6). Subfraction A1 was purified by recrystallization to give compound **1** as white crystals (6.02 g, 10.03% w/w). Subfraction A3 (1.53 g) was further fractionated by column chromatography (CC) using silica gel and washed with gradient eluents of chloroform, ethyl acetate and methanol to afford 5 subfractions (A3/1-A3/5). Subfraction A3/2 was then separated by preparative TLC using chloroform to obtain compound **4** as white needles (9.1 mg, 0.0152% w/w). Subfraction A3/4 was further isolated by VLC, and was then purified by Sephadex LH-20 using methanol as eluent is finally obtain compound **7** (yellow powder, 7.5 mg, 0.0125% w/w) and compound **8** (yellow powder, 8.9 mg, 0.0148% w/w), respectively.

Fraction B (2.06 g) was separated by VLC using silica gel and eluted with chloroform and with ethyl acetate and methanol, successively to afford 6 subfractions (B1-B6). Subfraction B1 was then purified by recrystallization to give compound **2** as white needles (352.4 mg, 0.587% w/w). Fraction B4 was further subjected to silica gel CC and eluted with 20% ethyl acetate in chloroform and with ethyl acetate to obtain compound **5** as a yellow powder (434.8 mg, 0.724% w/w). Fraction C (1.36 g) was separated by VLC using chloroform then with methanol as eluent to obtain four subfractions (C1-C4). Subfraction C2 was further purified by recrystallization to give compound **3** as a white amorphous material (42.8 mg, 0.0713% w/w). Subfraction C4 was subjected to silica gel CC and washed with gradient eluents of chloroform and methanol which finally afforded compound **6** as a beige powder (212.2 mg, 0.3536% w/w).

Table 1. Inhibition on HIV-1 IN activity of the fractions of *D. bulbifera* bulbils

Samples	% Inhibition at various concentrations (µg/mL)					IC_{50} (µg/mL)
	1	3	10	30	100	
$CHCl_3$ fraction	8.48±0.48	19.67±2.58	90.83±1.18	96.97±1.01	102.42±3.26	5.42
EtOAc fraction	1.82±0.81	7.70±5.15	93.64±0.05	97.76±0.76	101.21±3.22	6.49
H_2O fraction	6.65±0.15	10.49±2.64	47.48±7.71	95.44±0.36	98.53±4.04	9.12

Each value represents mean ± S.E.M. of four determinations.

The structures of compounds **1-8** were elucidated by spectroscopic methods including EIMS, 1D and 2D NMR analysis and also confirmed by comparison with data in the literature.

2.4 Assay of HIV-1 IN inhibitory activity

The inhibitory effect on HIV-1 IN activity by MIA was performed according to the method described by Tewtrakul *et al.* (2002). Suramin, an HIV-1 IN inhibitor, was used as a positive control. The % inhibition against HIV-1 IN was calculated as follows:

% inhibition against HIV-1 IN =
[(OD control – OD sample) / OD control] × 100

Where OD = absorbance detected from each well.

2.5 Molecular docking method

Ligand preparation

The three-dimensional structure of pure compounds was generated using the HyperChem professional 8.0. For each compound, geometry optimization was performed using the semi-empirical PM3 method. Before docking, the Gasteiger charges were assigned to each compound.

Integrase preparation

The crystal structure of the core domain of HIV-1 IN was obtained from the Protein Data Bank (PDB code 1QS4). IN was prepared according to the method previously reported (Vajragupta *et al.*, 2005). The second Mg^{2+} was placed in the same relative position according to the two metal structures of the Prototype Foamy Virus IN (PDB code 3OYA), a high structural homolog to HIV-1 IN (Krishnan and Engelman, 2012).

Docking

Molecular docking was performed with the AutoDock 4.2 program. The center of the grid boxes was set on the location of the co-crystallized inhibitor. The grid dimension was set to 60 x 60 x 60 $Å^3$ with a grid spacing of 0.375 Å. The docking calculations were carried out using the Lamarckian genetic algorithm (LGA). The optimized docking parameters were set as follows: the number of the GA runs was 100, the population size was 150, the maximum number of energy evaluations was increased to 2,500,000 per run and the maximum number of generations in the genetic algorithm was increased to 100,000. All other docking parameters were set at their default value. All 100 independent conformations for each compound with the root mean square deviation (RMSD) of less than 2 Å were clustered together. The best docked conformations were the lowest binding energy and the greatest number of conformations in the cluster (Healy *et al.*, 2009).

2.6 Statistical analysis

For statistical analysis, the results of the anti-HIV-1 IN activity were expressed as a mean value ± S.E.M. from four determinations. The IC_{50} values were calculated using the Microsoft Excel program.

3. Results and Discussion

A chloroform fraction of *D. bulbifera* bulbils extract was separated using column chromatography to give eight compounds (Figure 1), which were one new clerodane diterpenoid (diosbulbin E acetate, **4**), an epimer of 8-epidiosbulbin E acetate (**1**; Shriram *et al.*, 2008), together with 15,16 epoxy-6α-*O*-acetyl-8β-hydroxy-19-nor-clero-13(16),14-diene-17,12; 18,2-diolide (**2**; Kidyu *et al.*, 2011), sitosterol-β-D-glucoside (**3**; Viswanadh *et al.*, 2006), 3,5-dimethoxy-quercetin (**5**), (+)-catechin (**6**; Hye *et al.*, 2009), quercetin (**7**; Couladis *et al.*, 2002) and kaempferol (**8**; Hadizadeh *et al.*, 2003).

Compound **4** was a colourless amorphous solid, $C_{21}H_{24}O_7$, *m/z*: 329.7 $[M]^+$, $[\alpha]_D^{20}$ -5° (*c* 0.07, CHCλ₃), UV (CH₃OH) lmax: 215, 250, 347 nm. The IR spectrum indicated the presence of carbonyl groups (1773 and 1737 cm^{-1}) and a furan moiety (1505 and 875 cm^{-1}). The analytical NMR data are shown in Table 2 and compared with those of compound **1**. The ^1H NMR spectrum of compound **4** displayed the characteristic signal of a furan ring at δ 6.40 (H-14), 7.41 (H-15), 7.46 (H-16) and two methyl singlet signals at δ 2.10 (H-20) and 0.99 (H-21). Furthermore, oxygenated methine protons were observed as downfield signals at δ 4.82 (H-2), 5.44 (H-6) and 5.38 (H-12). Analysis of the ^{13}C NMR and DEPT spectra exhibited resonances of 21 carbons. Among these, three ester carbonyl groups were observed at δ 173.5 (C-17), 176.1 (C-18) and 170.8 (C-19). The signals exhibited at δ 143.8 (C-15), 139.5 (C-16), 124.0 (C-13) and 108.4 (C-14) were from the furan ring (Kapingu *et al.*, 2000), which indicated that this compound is a furano-clerodane diterpenoid. From the HMBC spectrum, the δ-lactone C=O at $δ_C$ 173.5 was assigned to a lactone at C-17 because it correlated with the protons at $δ_H$ 2.96 (H-8). The lactone C=O signal at $δ_C$ 176.1 was assigned at C-18 because of its correlation with protons at $δ_H$ 2.46 (H-3α), 1.80 (H-5) and 4.82 (H-2), which indicated that the lactone ring closure was at C-2. Similarly the third C=O signal at $δ_C$ 170.8 was assigned to a C-19, closer to C-6, due to the correlation with the methyl protons at $δ_H$ 2.10 (H-20). On the other hand, the methyl protons at $δ_H$ 0.99 (CH₃-21) were correlated with carbons at $δ_C$ 35.7 (C-9) and 40.8 (C-10) indicating this methyl group was linked to C-9. Furthermore, the furan ring was linked to C-12 and this was indicated by the quaternary carbon of this ring at $δ_C$ 124.0 (C-13) that correlated with the protons at $δ_H$ 5.38 (H-12) and 2.18 (H-11α).

The relative stereochemistry of **4** was determined using the NOESY spectrum and splitting pattern by comparison with **1**. Compound **1** showed a correlation between H-1α, H-2 and H-3α, and also between H-4, H-6 and H-5. Moreover,
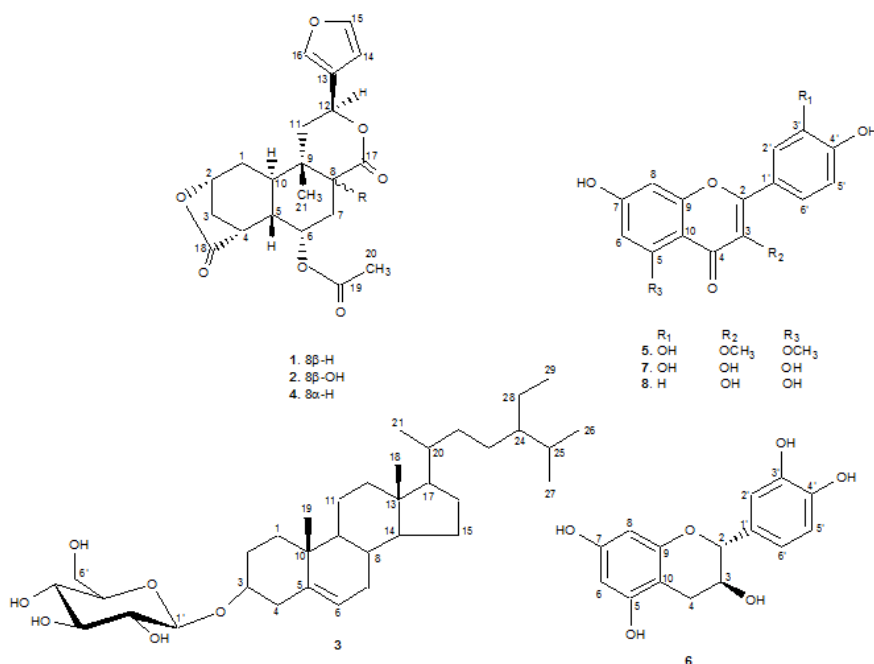
Figure 1. The structures of compounds isolated from *D. bulbifera* L. bulbils (1:8-Epidiosbulbin E acetate; 2: 15,16-Epoxy-6α-*O*-acetyl-8β-hydroxy-19-nor-clero-13(16),14-diene-17,12;18,2-diolide; 3: Sitosterol-β-D-glucoside; 4: Diosbulbin E acetate; 5: 3, 5-Dimethoxy-quercetin; 6: (+)-Catechin; 7: Quercetin; 8: Kaempferol)

Table 2. ^{1}H and ^{13}C NMR data in CDCl$_3$ of 8-epidiosbulbin E acetate (1) and diosbulbin E acetate (4) (500 MHz for ^{1}H)

| Position	8-Epidiosbulbin E acetate (1)				Diosbulbin E acetate (4)			
	δ_C	δ_H	Mult.	*J* (Hz)	δ_C	δ_H	Mult.	*J* (Hz)
1α	28.2	2.10	m	-	28.6	2.08	m	-
1β		1.44	dd	12.9, 12.3		1.39	d	6.0
2	76.4	4.85	dd	5.4, 5.1	76.3	4.82	dd	5.8, 5.3
3α	38.5	2.50	m	-	39.0	2.46	ddd	12.8, 5.8, 5.8
3β		1.74	d	11.5		1.74	d	12.8
4	42.0	2.56	dd	5.8, 0.8	41.5	2.64	d	5.8
5	41.1	1.90	ddd	12.5, 2.3, 0.8	42.1	1.80	m	-
6	69.1	5.13	ddd	2.6, 2.4, 2.3	68.6	5.44	ddd	3.5, 3.0, 3.0
7α	26.7	2.82	ddd	15.1, 2.6, 2.2	27.2	2.08	m	
7β		1.87	ddd	15.1, 6.1, 2.4		1.86	ddd	12.5, 12.5, 3.0
8	45.8	2.30	dd	6.1, 2.2	41.8	2.96	dd	12.5, 3.5
9	34.4	-	-	-	35.7	-	-	-
10	31.5	2.54	ddd	12.5, 12.3, 5.6	40.8	2.26	ddd	14.0, 12.0, 6.0
11α	39.6	2.10	m	-	42.1	2.18	dd	14.0, 6.0
11β		1.76	dd	12.6, 12.6		1.80	m	-
12	69.6	5.50	dd	12.6, 3.1	70.1	5.38	dd	12.6, 6.0
13	124.7	-	-	-	124.0	-	-	-
14	108.3	6.40	dd	1.7, 0.7	108.4	6.40	dd	2.0, 1.0
15	143.7	7.39	dd	1.7, 0.7	143.8	7.41	dd	2.0, 1.0
16	139.8	7.47	dd	0.7, 0.7	139.5	7.46	dd	1.0, 1.0
17	170.8	-	-	-	173.5	-	-	-
18	175.8	-	-	-	176.1	-	-	-
19	170.7	-	-	-	170.8	-	-	-
20	20.8	1.98	s	-	21.2	2.10	s	-
21	21.8	1.11	s	-	21.2	0.99	s	-
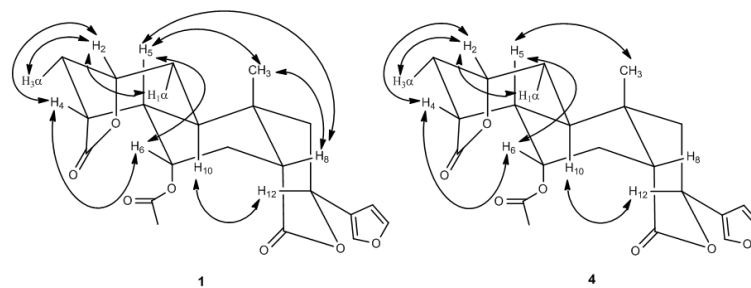
Figure 2. NOESY correlations of compounds 1 and 4.

H-5 showed a correlation with CH$_3$-21 and H-8. In particular, the lack of correlation between H-5 and H-10 indicated that they were in a trans-configuration, while H-10 showed a correlation with H-12 to indicate that these two protons were in the cis-configuration (Figure 2). It is clearly indicated that the relative stereochemistry of C-2, C-4, C-5, C-6, C8, C-10, C-12 and CH$_3$-21 positions, led to the relative configuration proposed for **1** (Figure 1). In the case of compound **4**, the correlations that were observed between H-5 and CH$_3$-21 indicated that they were in the same orientation as in that of compound **1**. It was of interest that H-8 showed no correlation with CH$_3$-21 while it was observed in compound **1** (Figure 2). This led to a proposal for the stereochemistry of H-8 that it was in the α-orientation.

The splitting pattern and coupling constant of **4** was similar to that of **1** as observed at H-2, H-6, H-10 and H-12 but the main differences between the two compounds was the coupling constants of H-8. Compound **1** displayed two small coupling constants (dd, J = 6.1, 2.2 Hz) while compound **4** displayed one large and one small coupling constants (dd, J = 12.5, 3.5 Hz) due to its α-H orientation with H-8 in **4**, instead of β-H as in **1**. These data were also in good agreement with the coupling constants of 8-epidiosbulbin E (dd, J = 6.3, 2.1 Hz; 8β-H) and its epimer, diosbulbin E (dd, J = 12.2, 3.6 Hz; 8α-H) (Rakotobe *et al.*, 2010).

Furthermore, when comparing **4** with **1,** the chemical shift of the C-7, C-8 and C-20 of **4** were shifted upfield by -0.4, -4.0 and -3.3 ppm, whereas the chemical shifts of C-9, C-10, C-11 and C-17 were shifted downfield by +1.3, +9.3, +2.5 and +2.7 ppm, respectively. It was of interest that a change from 8β-H to 8α-H resulted in a shift downfield of about +10 ppm for C-10 (Rakotobe *et al.*, 2010). Thus compound **4** differed from compound **1** in its configuration at C-8. The structure of compound **4** was established as 15, 16-epoxy-6α-*O*-acetyl-19-nor-clero-13(16),14-diene-17,12S; 18,2α-diolide, the epimer at C-8 of 8-epidiosbulbin E acetate (**1**), a compound previously isolated from the same plant. Therefore, compound **4** was named as diosbulbin E acetate.

The anti-HIV-1 IN activity of isolated compounds were determined by the MIA and compared with suramin, a positive control (IC$_{50}$ = 2.24 μM, Table 3). Compounds **6-8**, were characterized as flavonoids, they exhibited a much higher anti-HIV-1 IN activity than the diterpenoid and the steroid compounds (**1-4**). Among the flavonoids, different inhibitory effects were observed for quercetin (**7**) that exhibited the strongest anti-HIV-1 IN activity with an IC$_{50}$ value of 16.28 μM, followed by kaempferol (**8**, IC$_{50}$ = 37.71 μM) and (+)-catechin (**6**, IC$_{50}$ = 62.36 μM) while 3,5-dimethoxyquercetin (**5**) were inactive (IC$_{50}$ > 100 μM). 8-Epidiosbulbin E acetate (**1**, IC$_{50}$ = 70.39 μM) and diosbulbin E acetate (**4**, IC$_{50}$ = 73.49

Table 3. Anti-HIV-1 IN activity of pure compounds from *Dioscorea bulbifera* L. bulbils

Compounds	% Inhibition at various concentrations (μM)					IC$_{50}$ (μM)
	1	3	10	30	100	
8-Epidiosbulbin E acetate (1)	-	-	29.42 ± 3.34	36.48 ± 2.25	59.99 ± 0.54	70.39
15,16-Epoxy-6α-O-acetyl-8β-hydroxy-19-nor-clero-13(16),14-diene-17,12;18,2-diolide (2)	-	-	26.45 ± 2.33	30.85 ± 0.89	38.21 ± 0.44	>100
Sitosterol-β-D-glucoside (3)	-	-	37.97 ± 2.33	43.78 ± 2.26	45.62 ± 0.61	>100
Diosbulbin E acetate (4)	-	-	32.36 ± 1.68	39.47 ± 2.63	57.98 ± 1.54	73.45
3, 5-Dimethoxyquercetin (5)	-	-	35.60 ± 2.03	34.93 ± 0.70	40.93 ± 1.83	>100
(+)-Catechin (6)	-	27.65 ± 5.66	31.22 ± 0.63	34.23 ± 0.94	66.19 ± 1.47	62.36
Quercetin (7)	-	34.85 ± 2.60	48.06 ± 0.90	53.98 ± 1.62	65.15 ± 1.18	16.28
Kaempferol (8)	-	-	36.86 ± 1.23	45.75 ± 3.66	61.36 ± 0.90	37.71
Suramin (positive control)	35.26 ± 0.58	55.19 ± 0.91	74.18 ± 0.20	91.42 ± 0.38	100.51 ± 0.70	2.24

Each value represents mean S.E.M. of four determinations.

µM) also showed moderate inhibition against the IN enzyme, whereas 15,16-epoxy-6α-*O*-acetyl-8β-hydroxy-19-nor-clero-13(16),14-diene-17,12; 18,2-diolide (**2**) and sitosterol-β-D-glucoside (**3**) were inactive (IC$_{50}$ > 100 µM). The inhibitory effect of quercetin (**7**) and sitosterol-β-D-glucoside (**3**) are in agreement with our previous results (Bunluepuech *et al.*, 2013; Kejik, 2007). These bioassay results indicated that hydroxylated aromatic compounds, especially compounds bearing the catechol group, were required for effective IN inhibition. For the cytotoxic activity, (+)-catechin, quercetin and kaempferol possessed cytotoxic effect against human cancer cell lines (Costa-Lotufo *et al.*, 2003; Shen *et al.*, 2003; Evacuasiany et al., 2014) but there have been no report on the cytotoxic activity in normal cells of the isolated compounds of *D bulbifera*.

      In order to investigate the interactions of the active compounds with the IN, molecular docking calculations were carried out to predict the receptor-ligand interactions. In an effort to validate the docking protocol, we also docked against 5CITEP, the inhibitor, with the core domain of HIV-1 IN to reproduce the binding pose. The result showed that the redocked inhibitor was perpendicular to the pose of the co-crystallized inhibitor (Figure 3). In this case, the reason for these different orientations in the binding site related to the crystal packing effect in the crystal structure can influence the position of the inhibitor (Sotriffer, Ni and McCammon, 2000).

      In this study, we investigated such interactions for all four flavonoids (**5-8**). The docking results showed that the binding energy of compounds **7** and **8** (-5.90 and -5.83 kcal/mol, respectively) were lower than those of compounds **6** and **5** (-5.16 and -4.98 kcal/mol, respectively). This indicated that **7** and **8** interacted more strongly with the IN. This result was consistent with their activity as determined by the MIA method, in which there was a relationship between the binding energy and the inhibitory potency against HIV-1 IN. Although compounds **5-8** revealed non-significant numbers of estimated binding energy, the interacting amino acid residues were different. Mostly, the differences of binding interactions as well as the numbers of hydrogen bond were the major aspects that were reflected in the activity of each compound.

      According to Figure 4, compound **7** which is the most active compound was found to locate in the active site. It formed five hydrogen bonds with Thr66, His67, Lys159 including a tight binding with two hydrogen bonds with Glu152, the catalytic residue of IN (Figure 4A). Compound **8** had a similar inhibitory mechanism to compound **7**. It interacted with Thr66, His67, Glu152, Lys159 and also bound with Gln148 (Figure 4B), a flexible loop which is essential for HIV-1 IN activity (Greenwald *et al.*, 1999). Thus, altering the flexibility of the loop (Gly140-Gly149) could lead to an inhibition of IN activity (Jiang *et al.*, 2010). In the case of compound **6**, it showed weaker interactions with the IN active site in terms of the lower number of hydrogen bonds. Compound **6** was also found to locate close to the flexible
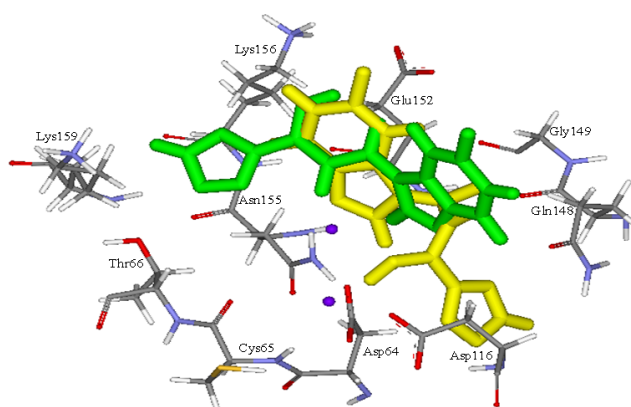

Figure 3. Superimposed structures of redocked inhibitor (yellow) and the co-crystallized inhibitor (green) in the core domain of HIV-1 IN. The relative residues are stick models and colored by heteroatoms, whereas the Mg^{2+} is purple balls.
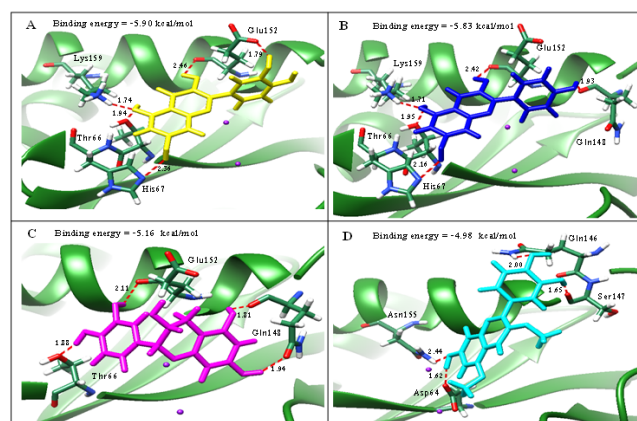

Figure 4. Molecular docking of the flavonoid compounds with HIV-1 IN. The ribbon model shows the backbone of the HIV-1 IN catalytic domain with all interacting amino acid residues shown as stick models and colored by heteroatoms. Compound 7 (A), compound 8 (B), compound 6 (C) and compound 5 (D). Mg^{2+} (purple balls), H-bond interactions (red dashed lines), represent bond length in angstroms (Å).

loop that was slightly different from compounds **7** and **8**. Compound **6** formed two hydrogen bonds with Thr66, Glu152 and two hydrogen bonds with Gln148 (Figure 4C). On the other hand, compound **5** that was substituted with two methoxy groups, was inactive (IC$_{50}$ > 100 µM). The orientation of this compound is remarkably different from the active compounds that can be observed in Figure 5. It moved far away from the catalytic residue Glu152 and was oriented towards the Gln146 and Ser147, and formed hydrogen bonds with these two amino acids as well as with Asp64 and Asn155 (Figure 4D). Therefore, the results could be used to explain why compound **5** was inactive against the IN target, as it lacked an interaction with the catalytic residue Glu152. The binding mode from this docking study was in good agreement
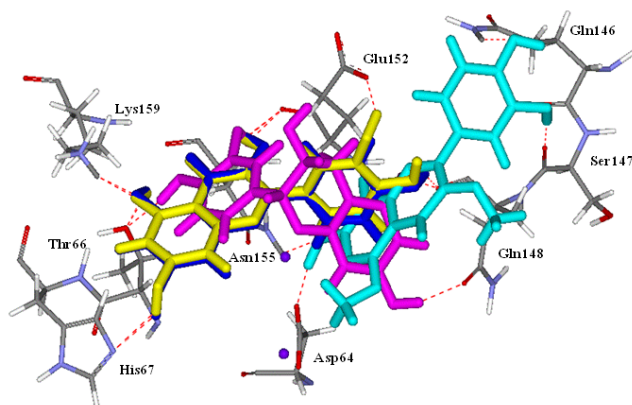
Figure 5. Superimposed structures of the flavonoid compounds; compound 5 (aqua), compound 6 (magenta), compound 7 (yellow) and compound 8 (blue) with the IN amino acid residues (small stick). Mg^{2+} (purple balls), H-bond interactions (red dashed lines), represent bond length in angstroms (Å).

with its biological activity. These docking results indicated that the hydroxyl group played an important role in the binding to the amino acid residues in the IN active site. This is in agreement with the previous report (Lameira *et al.*, 2006). It was important that the active compounds were found to strongly interact with Lys159, Thr66, His67, Gln148 and Glu152. Accordingly, these five residues are suggested to be very significant for their inhibitory action against IN.

In conclusion, from the present study, one new clerodane diterpene (**4**), two clerodane diterpenoids (**1-2**), four flavonoids (**5-8**) and one sterol glucoside (**3**) were isolated from the bulbils of *D. bulbifera*. Based on the anti-HIV-1 IN activity of the compounds from *D. bulbifera*, the bulbils of this plant have potential for AIDS treatment. Moreover, the structural models of the interactions at the IN active site are useful for the future design of HIV-1 IN inhibitors.

Acknowledgements

References

Ahmed, Z., Chishti, M.Z., Johri, R.K., Bhagat, A., Gupta, K.K., and Ram, G. 2009. Antihyperglycemic and anti-dyslipidemic activity of aqueous extract of *Dioscorea bulbifera* tubers. Diabetologia Croatica. 38(3), 63-72.

Asante-Appiah, E. and Skalka, A.M. 1997. Molecular mechanisms in retrovirus DNA integration. Antiviral Research. 36, 139-156.

Bunluepuech, K., Wattanapiromsakul, C., Madaka, F., and Tewtrakul, S. 2013. Anti-HIV-1 integrase and anti-allergic activities of *Bauhinia strychnifolia*. Songklanakarin Journal of Science and Technology. 35(6), 659-664.

Camarasa, M.J., Velazquez, S., San-Felix, A., Perez-Peez, M.J., and Gago, F. 2006. Dimerization inhibitors of HIV-1 reverse transcriptase, protease and integrase: A single mode of inhibitor for the three HIV enzymes? Antiviral Research. 71, 260-267.

Clercq, E.D. 2009. Anti-HIV drugs: 25 compounds approved within 25 years after the discovery of HIV. International Journal of Antimicrobial Agents. 33, 307-320.

Couladis, M., Baziou, P., Verykokidou, E., and Loukis, A. 2002. Antioxidant activity of polyphenols from *Hypericum triquetrifolium* Turra. Phytotherapy Research. 16, 769-770.

Goldgur, Y., Craigie, R., Cohen, G.H., Fujiwara, T., Yoshinaga, T., Fujishita, T., Sugimoto, H., Endo, T., Murai, H., David, R., and Davie, D.R. 1999. Structure of the HIV-1 integrase catalytic domain complexed with an inhibitor: A platform for antiviral drug design. Proceedings of the National Academy of Sciences of the United States of America. 96, 13040-13043.

Costa-Lotufo, L.V., Jimenez, P.C., Wilke, D.V., Leal, L.K.A.M., Cunha, G.M.A., Silveira, E.R., Canuto, K.M., Viana, G.S.B., Moraes, M.E.A., Moraes, M.O., and Pessoa, C. 2003. Antiproliferative effects of several compounds isolated from *Amburana cearensis* A.C. Smith. Journal for Nature Research. 58c, 675-680.

Evacuasiany, E., Ratnawati, H., Liana, L.K., Widowati, W., Maesaroh, M., Mozef, T., and Risdian, C. 2014. Cytotoxic and antioxidant activities of catechins in inhibiting the malignancy of breast cancer. Oxidants and Antioxidants in Medical Science. 3(2), 141-146.

Greenwald, J., Le, V., Butler, S.L., Bushman, F.D., and Choe, S. 1999. The mobility of an HIV-1 integrase active site loop is correlated with catalytic activity. Biochemistry. 38, 8892-8898.

Hadizadeh, F., Khalili, N., Hosseinzadeh, H., and Khair-Aldine, R. 2003. Kaempferol from Saffron petals. Iranian Journal of Pharmaceutical Research. 2, 251-252.

Healy, E.F., Sanders, J., Peter, J., King, P.J., and Robinson Jr, W.E. 2009. A docking study of L-chicoric acid with HIV-1 integrase. Journal of Molecular Graphics and Modelling. 27, 584-589.

Hye, M.A., Taher, M.A., Ali, M.Y., Ali, M.U., and Zaman, S. 2009. Isolation of (+)-catechin from *Acacia catechu* (Cutch Tree) by a convenient method. Journal of Scientometric Research. 1(2), 300-305.

Jiang, F., Chen, W., Yi, K., Wu, Z., Si, Y., Han, W., and Zhao, Y. 2010. The evaluation of catechins that contain a galloyl moiety as potential HIV-1 integrase inhibitors. Clinical Immunology. 137, 347-356.

Kapingu, M.C., Guillaume, D., Mbwambo, Z., Moshi, M.J., Uliso, F.C., and Muhunnah, R.L.A. 2000. Diterpenoids from the roots of *Croton macrostachys*. Phytochemistry. 54, 767-770.

Katz, R.A. and Skalka, A.M. 1994. The retroviral enzymes. Annual Review of Biochemistry. 63, 133-173.

Kejik, R. 2007. Study on antioxidant activity and HIV-1 integrase inhibitory effect of *Smilax corbularia* Kunth. Master of Pharmacy in Pharmaceutical Sciences. Prince of Songkla University, Thailand.

Kidyu, K., Thaisuchat, H., Meepowpan, P., Sukdee, S., Nuntasaen, N., Punyanitya, S., and Pompimon, W. 2011. New clerodane diterpenoid from the bulbils of *Dioscorea bulbifera*. Natural Product Communications. 6(8), 1069-1072.

Krishnan, L., and Engelman, A. 2012. Retroviral integrase proteins and HIV-1 DNA integration. The Journal of Biological Chemistry. 287, 40858-40866.

Lameira, J., Medeiros, I.G., Reis, M., Santos, A.S., and Alves, C.N. 2006. Structure activity relationship study of flavone compounds with anti-HIV-1 integrase activity: A density functional theory study. Bioorganic and Medicinal Chemistry. 14, 7105-7112.

Mbiantcha, M., Kamanyi, A., Teponno, R.B., Tapondjou, A.L., Watcho, P., and Nguelefack, T.B. 2011. Analgesic and anti-inflammatory properties of extracts from the bulbils of *Dioscorea bulbifera* L. var *sativa* (Dioscoreaceae) in mice and rats. Journal of Evidence-Based Complementary and Alternative Medicine. 2011, 1-9.

Rakotobe, L., Mambua, L., Deville, A., Dubost, L., Jeannoda, V., Rakoto, D., and Bodo, B. 2010. Clerodane and 19-norclerodane diterpenoids from the tubers of *Dioscorea antaly*. Phytochemistry. 71, 1007-1013.

Saag, M.S. 2012. New and investigational antiretroviral drugs for HIV infection: mechanisms of action and early research findings. Topics in Antiviral Medicine. 20(5), 162-167.

Shen, S.C., Chen, Y.C., Hsu, F.L., and Lee, W.R. 2003. Differential apoptosis-inducing effect of quercetin and its glycosides in human promyeloleukemic HL-60 cells by alternative activation of the caspase 3 cascade. Journal of Cellular Biochemistry. 89, 1044-1055.

Shriram, V., Jahagirdar, S., Latha, C., Kumar, V., Puranik, V., Rojatkar, S., Dhakephalkar, P.K., and Shitole, M.G. 2008. A potential plasmid-curing agent, 8-epidiosbulbin E acetate from *Dioscorea bulbifera* L. against multi-drug-resistant bacteria. International Journal of Antimicrobial Agents. 32, 405-410.

Sotriffer, C.A., Ni, H., and McCammon, J.A. 2000. HIV-1 integrase inhibitor interactions at the active site: prediction of binding modes unaffected by crystal packing. Journal of the American Chemical Society. 122, 6136-6137.

Tewtrakul, S., Nakamura, N., Hattori, M., Fujiwara, T., and Supavita, T. 2002. Flavanone and flavonol glycosides from the leaves of *Thevetia peruviana* and their HIV-1 reverse transcriptase and HIV-1 integrase inhibitory activities. Chemical and Pharmaceutical Bulletin. 50, 630-635.

Vajragupta, O., Boonchoong, P., Morrisc, G.M., and Olsonc, A.J. 2005. Active site binding modes of curcumin in HIV-1 protease and integrase. Bioorganic & Medicinal Chemistry Letters. 15, 3364-3368.

Viswanadh, G.S., Ramaiah, P.A., Laatsch, H., and Maskey, R. 2006. Chemical constituents of the heartwood and bark of *Homononia riparia*. Journal of Tropical Medicinal Plants. 7(2), 267-273.

Wang, J.M., Ji, L.L., Branford-White, C.J., Wang, Z.Y., Shen, K.K., Liu, H., and Wang, Z.T. 2012. Antitumor activity of *Dioscorea bulbifera* L. rhizome in vivo. Fitoterapia. 83, 388-394.